Triple-differential cross sections for electron-impact ionization of helium*

D. H. Madison and R. V. Calhoun
Department of Physics, Drake University, Des Moines, Iowa 50311

W. N. Shelton
Department of Physics, Florida State University, Tallahassee, Florida 32306

(Received 10 March 1977)

Triple-differential cross sections for electron-impact ionization of helium are calculated in the distorted-wave approximation. A general distorted-wave formalism for ionization is presented for two coordinate systems—one with the z axis parallel to the direction of the incident electron and one with the z axis parallel to the momentum-transfer direction. Cross sections in the scattering plane are compared with experimental results and with other theoretical calculations. Cross sections out of the scattering plane are presented and spatial symmetries are discussed.

I. INTRODUCTION

The problem of atomic charged particle scattering has been studied experimentally and theoretically since the 1920's. Until recently, the experimental cross sections have been analyzed using elementary first-order theories such as the plane-wave Born approximation (PWBA). However, with improved experimental techniques, more detailed ionization cross sections have been measured which cannot be explained using these theories. Recently Erhardt *et al.*,[1-4] Hood *et al.*,[5] and Wiegold[6] have measured triple-differential cross sections for electron-impact ionization. The study of triple-differential cross sections for ionization represents a fundamental testing ground for different theoretical approaches, since the collision dynamics are completely specified. Various theoretical calculations for electron-impact ionization of helium have been performed in the PWBA,[7-10] the Coulomb-projected Born approximation (CPBA),[11] and the many-body Green's function approach.[12]

In this paper, we report the results of a distorted-wave calculation. This work represents an extension to the ionization problem of previous distorted-wave calculations for excitation.[13-15] A general distorted-wave approximation (DWA) theory for ionization is outlined in Sec. II. Specific results are given for two-coordinate systems of particular interest: (i) z axis parallel to the direction of the incident electron, and (ii) z axis parallel to the momentum-transfer direction. The latter system is of particular interest since the PWBA predicts an azimuthal symmetry about this direction. In Sec. III, the results of the calculation in the scattering plane are compared with experimental data and previous theoretical calculations. The DWA results off the scattering plane are also presented and symmetries are discussed.

The distorted-wave formalism developed in Sec. II is more complex than is needed to treat ionization of the helium atom. However, it is sufficiently general to treat a wide variety of systems, and will preclude the necessity of introducing a new formalism for more complex systems.

II. THEORY

The triply differential cross section for ionization is given in atomic units by

$$\frac{d\sigma}{d\Omega_f\, d\Omega_s\, dE} = \frac{(2\pi)^4}{E_i} \sum_{\text{ave}} |T|^2 , \tag{1}$$

where E_i is the energy of the incident electron, Ω_f (Ω_s) is the solid angle of observation for the fast (slow) final-state continuum electron, dE is the energy interval for one of the final-state energy-normalized continuum electrons, and the summation and average imply summing over final, and averaging over initial, indistinguishable states. In the distorted-wave approximation, the T matrix for electron-impact ionization including exchange is given by

$$T_{ba} = \left\langle \phi_f^{(-)}(1)\psi_b(2,\ldots,N+1) \left| \sum_{i=2}^{N+1} \frac{2}{r_{i1}} - V_f(1) \right| \left(1 - \sum_{j=2}^{N+1} P_{j1} \right) \phi_a^{(+)}(1)\psi_a(2,\ldots,N+1) \right\rangle , \tag{2}$$

where ψ_a is the properly antisymmetrized wave function for the atom in its initial state, ψ_b is the properly antisymmetrized wave function for the final-state ion plus slow electron, ϕ_a is the incident-electron distorted wave, ϕ_f is the distorted wave representing the fast electron, and P_{ij} is

the operator that interchanges electrons i and j. The distorted waves ϕ_a and ϕ_f are calculated as eigenfunctions of the Hamiltonian

$$H_D = T - 2Z/r + V_f , \tag{3}$$

where T is the kinetic energy operator of the incident electron and Z is the charge on the atomic nucleus. The potential V_f is the spherical average of the interaction between the incident electron and the atomic electrons; a first approximation to this potential may be obtained from a Hartree-Fock bound-state calculation. Note that we employ the prior form of the interaction due to the relative simplicity of the initial state of the system. The plane-wave Born approximation (PWBA)[16] is obtained if the last two terms of (3) are set equal to zero and the exchange terms are dropped.

Each of the N interchange terms gives an identical contribution to (2) due to the fact that particles 2 through $N+1$ contribute to the matrix element in a completely symmetric fashion. Using this fact, the T matrix becomes

$$\begin{aligned} T_{ba} = {} & \langle \phi_f^{(-)}(1)\psi_b(2,\ldots,N+1) \mid \sum_{i=2}^{N+1} \frac{2}{r_{i1}} \\ & - V_f(1) \mid \phi_a^{(+)}(1)\psi_a(2,\ldots,N+1)\rangle \\ & - N \langle \phi_f^{(-)}(1)\psi_b(2,\ldots,N+1) \mid \sum_{i=2}^{N+1} \frac{2}{r_{i1}} \\ & - V_f(1) \mid \phi_a^{(+)}(2)\psi_a(1,3,\ldots,N+1)\rangle . \end{aligned} \tag{4}$$

Within the single-electron picture, ψ_a (ψ_b) is composed of a properly antisymmetrized combination of single-particle orbitals such as a Slater determinant or some linear combination of Slater determinants; ψ_a is composed entirely of bound states while ψ_b contains one continuum state. If one adopts the viewpoint that the slow electron is scattered primarily by the atomic field, the bound and continuum wave functions would be eigenfunctions of an effective (Hartree-Fock) potential for the atom.

A first approximation to the effective (Hartree-Fock) one-electron potential for the active electron may be obtained from the charge distribution of the (frozen) ionic core. The electronic contribution V_s to this potential differs from V_f in that V_f results from the charge distribution of N electrons and V_s from $N-1$ electrons. If all the single-particle wave functions comprising ψ_a (ψ_b) are calculated as eigenfunctions of the same effective potential, they are all orthogonal. As a result of this orthogonality, the V_f term in the first matrix element (direct-scattering) of (4) vanishes. To illustrate the various different types of terms in the T matrix, we have evaluated the amplitudes for the specific case in which ψ_a (ψ_b) is represented by a single Slater determinant[17]:

$$T_{ba} = T_{\rm dir} - T_{\rm ex} , \tag{5}$$

where $T_{\rm dir}$ and $T_{\rm ex}$ are the direct and exchange T matrices, respectively, and where

$$T_{\rm dir} = N \langle \phi_f^{(-)}(1)\psi_b(2,\ldots,N+1) \mid 2/r_{12} \mid \phi_a^{(+)}(1)\psi_a(2,\ldots,N+1)\rangle \tag{6}$$

and

$$\begin{aligned} T_{\rm ex} = {} & \langle \phi_f^{(-)}(1) \mid V_f(1) \mid \chi_N(1)\rangle \langle \phi_s^{(-)}(2) \mid \phi_a^{(+)}(2)\rangle \\ & + \sum_{j=1}^{N-1} \langle \chi_j(3) \mid \phi_a^{(+)}(3)\rangle \langle \phi_f^{(-)}(1)\phi_s^{(-)}(2) \mid 2/r_{12} \mid [\chi_j(1)\chi_N(2) - \chi_j(2)\chi_N(1)]\rangle \\ & + \sum_{j=1}^{N-1} \langle \phi_s^{(-)}(3) \mid \phi_a^{(+)}(3)\rangle \langle \phi_f^{(-)}(1)\chi_j(2) \mid 2/r_{12} \mid [\chi_j(2)\chi_N(1) - \chi_j(1)\chi_N(2)]\rangle \\ & + \langle \phi_f^{(-)}(1)\phi_s^{(-)}(2) \mid 2/r_{12} \mid \chi_N(1)\phi_a^{(+)}(2)\rangle . \end{aligned} \tag{7}$$

Here, the single-particle wave functions χ and ϕ_s are eigenfunctions of the Hamiltonian

$$H_A = T - 2Z/r + V_s . \tag{8}$$

The terms of (7) correspond to various modes of exchange. The first term is produced by the electronic potential V_f and corresponds to exchange between the incident electron (defined as the electron initially in the state $\phi_a^{(+)}$) and the active electron (defined as the electron initially in the state χ_N, which is left vacant by the collision). The remaining terms originate from the two-particle operator, and may be given simple interpretations. The second term of (7) is the "electron-capture" term in which the initial electron is absorbed and remains as a constituent of the residual ion through replacement of a spectator electron, which must then be ejected. The two contributions to this term arise from the two possible ways in which this spectator electron and the active elec-

tron may be ejected into the two continuum states. In the third term of (7) the incident electron becomes the slow final-state continuum electron. The two contributions to this term arise from the two possible ways in which the fast final-state continuum electron may be produced—either by ejection of the active electron in the presence of a spectator, or by ejection of the spectator electron itself, the resultant vacancy in this latter case being filled by the active electron. Note that there is a sum over all possible spectator-electron states χ_j in the above two terms. In the last term of (7) the incident electron becomes the slow final-state continuum electron, while the active electron is ejected and becomes the fast final-state continuum electron.

It is this last term that is normally referred to as the exchange term. It is to be noted, however, that the first three terms will vanish only if the bound and continuum wave functions are orthogonal to ϕ_a. This orthogonality is not satisfied in the PWBA, since plane waves are not orthogonal to realistic atomic wave functions. This orthogonality is possible in the DWA and is imposed to make the calculation simpler.

Assuming this orthogonality, the exchange T matrix for arbitrary atomic wave functions becomes

$$T_{ex} = N\langle \phi_f^{(-)}(1)\psi_b(2,\ldots,N+1)|2/r_{12}|\phi_a^{(+)}(2)\psi_a(1,3,\ldots,N+1)\rangle , \tag{9}$$

which has a structure similar to that of the direct term (6).

To evaluate the direct and exchange T matrices, we make a fractional parentage expansion of the initial atomic wave function:

$$|\psi_a(2,\ldots,N+1)\rangle = \sum_{\alpha_p S_p L_p,\ \alpha_o l_o} \langle \alpha_p S_p L_p, \alpha_o l_o|\}\alpha LS\rangle \times \sum_{\substack{M_p m_o,\\ M_{s_p}\mu_o}} C(L_p l_o L; M_p m_o M_L) C(S_p S_o S; M_{s_p}\mu_o M_s) \times |\alpha_p L_p M_p, S_p M_{s_p}(3,\ldots,N+1)\rangle\, |\alpha_o l_o m_o; S_o \mu_o(2)\rangle . \tag{10}$$

Here $C(l_1 l_2 l_3; M_1 M_2 M_3)$ is a Clebsch-Gordan coefficient; the coefficient of fractional parentage[18] is $\langle \alpha_p S_p L_p, \alpha_o l_o|\}\alpha LS\rangle$; L and S are the quantum numbers of the initial atomic state; L_p and S_p are the total orbital and spin angular momentum of the parent; l_o is the orbital angular momentum of the active electron; α_p, α_o, and α are any additional quantum numbers necessary to describe the particular states completely; $|\alpha_p L_p M_p, S_p M_{s_p}\rangle$ represents the antisymmetrized wave function for the parent state; and $|\alpha_o l_o m_o; S_o \mu_o\rangle$ is the single-particle wave function for the active electron. In the same spirit, the final-state wave function is expressed as an antisymmetrized product of the residual core and slow-electron wave functions:

$$|\psi_b(2,\ldots,N+1)\rangle = N^{-1/2}\left(1 - \sum_{j=3}^{N+1} P_{2j}\right)|\phi_s^{(-)}(2)\rangle \times |\alpha_c L_c M_c;\ S_c M_{s_c}(3,\ldots,N+1)\rangle . \tag{11}$$

If these expansions are inserted into the T matrix, it is seen that

$$T = N^{1/2}\langle \alpha_c S_c L_c, \alpha_o l_o|\}\alpha LS\rangle\, C(L_c l_o L; M_c m_o M_L) \times C(S_c S_o S; M_{s_c}\mu_o M_s) \times (f\,\delta_{m_b m_a}\delta_{\mu_o m_e} - g\delta_{m_b \mu_o}\delta_{m_e m_a}), \tag{12}$$

where m_a (m_b) is the initial (final) spin projection of the projectile electron, $\mu_o(m_e)$ is the spin projection for the active electron, and

$$f = \langle \phi_f^{(-)}(1)|\langle \phi_s^{(-)}(2)|2/r_{12}|\phi_a^{(+)}(1)\rangle|\alpha_o l_o m_o(2)\rangle \tag{13}$$

and

$$g = \langle \phi_s^{(-)}(1)|\langle \phi_f^{(-)}(2)|2/r_{12}|\phi_a^{(+)}(1)\rangle|\alpha_o l_o m_o(2)\rangle . \tag{14}$$

The matrix elements f and g are of similar forms since both wave functions on the left-hand side represent continuum electrons. This result is equivalent to that obtained by Rudge.[19]

The cross section for an unpolarized beam incident on an unpolarized target is thus found to be

$$\frac{d\sigma}{d\Omega_f\, d\Omega_s\, dE} = \frac{(2\pi)^4}{E_i} N\langle \alpha_c S_c L_c, \alpha_o l_o|\}\alpha LS\rangle^2 \times (|f|^2 + |g|^2 - \mathrm{Re} f^* g) . \tag{15}$$

A. Evaluation of amplitude

To cast the direct and exchange amplitudes into a form suitable for evaluation, it is convenient to make a partial-wave decomposition of the amplitude. We can evaluate both the direct and exchange amplitudes at the same time if we look at a general amplitude of the form

$$t = \langle u_1^{(-)}(\vec{k}_m, \vec{r}_1) | \langle u_2^{(-)}(\vec{k}_n, \vec{r}_2) | 2/r_{12} \times | \phi_a^{(+)}(\vec{k}_i, \vec{r}_1) \rangle | \alpha_o l_o m_o(\vec{r}_2) \rangle , \quad (16)$$

where u_1 and u_2 are arbitrary continuum waves normalized to the proper boundary conditions implied by the wave number $\vec{k}$. The following convention is used for the wave numbers: $\vec{k}_i$ corresponds to the incident electron, while $\vec{k}_1$ ($\vec{k}_2$) corresponds to the fast (slow) final-state electron. If $m=1$ and $n=2$, (16) represents the direct amplitude, while an interchange of these values yields the exchange amplitude. The appropriate energy-normalized expansion for the continuum waves is

$$u^{(+)}(\vec{k}, \vec{r}) = (k\pi)^{-1/2} r^{-1} \sum_{lm} i^l \beta_l(k, r)\, Y_{lm}^*(\hat{k}) Y_{lm}(\hat{r}) , \quad (17)$$

where Y_{lm} is a spherical harmonic, a caret indicates the solid angle specifying the direction of a vector, and where

$$\beta_l(k, r) \xrightarrow[r\to\infty]{} e^{i\delta_l} \sin(kr - \tfrac{1}{2} l\pi + \delta_l) \quad (18)$$

if the particle is asymptotically in a field-free region, or

$$\beta_l(k, r) \xrightarrow[r\to\infty]{} e^{i(\sigma_l + \delta_l)} \sin[kr - k^{-1} \ln(2kr) - \tfrac{1}{2} l\pi + \sigma_l + \delta_l] \quad (19)$$

if the particle is asymptotically in a Coulombic field. Here σ_l is the Coulomb phase shift[20] and δ_l is the ordinary phase shift. The initial bound-state wave function is expressed as

$$| \alpha_o l_o m_o(\vec{r}) \rangle = i^{l_o} r^{-1} U_{l_o}(r) Y_{l_o m_o}(\hat{r}) . \quad (20)$$

When these expansions along with the multipole expansion for the Coulombic interaction are inserted into (16), it may be shown after some angular momentum algebra that the amplitude reduces to

$$t = 2(\pi^3 k_i k_1 k_2)^{-1/2} \sum_{l_1 m_1 l_2 m_2 l_i m_i l m} [(2l_i+1)(2l_1+1)(2l_o+1)(2l+1)^{-2}(2l_2+1)^{-1}]^{1/2} \times i^{l_o+l_i-l_1-l_2} I^{k_i k_m k_n}_{l_o l_i l_1 l_2} C(l_i l_1 l; m_i m_1 m)\, C(l_o l l_2; m_o m m_2) C(l_i l_1 l; 0) C(l_o l l_2; 0) \times Y^*_{l_1 m_1}(\hat{k}_m) Y_{l_2 m_2}(\hat{k}_n) Y^*_{l_i m_i}(\hat{k}_i) . \quad (21)$$

We have used the notation $C(l_1 l_2 l_3; 0)$ to mean $C(l_1 l_2 l_3; 000)$. The radial integral in (21) is

$$I^{k_i k_m k_n}_{l_o l_i l_1 l_2} = \int_0^\infty \beta^1_{l_1}(k_m, R) \beta^i_{l_i}(k_i, R) F^{k_n}_{l_o l l_2}(R)\, dR , \quad (22)$$

where

$$F^{k_n}_{l_o l l_2}(R) = \int_0^\infty \beta^2_{l_2}(k_n, r) \frac{r_<^l}{r_>^{l+1}} U_{l_o}(r)\, dr . \quad (23)$$

Here β^i_l is the radial component of the lth partial wave for the incident projectile, β^1_l (β^2_l) is the radial component for the lth partial wave associated with $u_1^{(-)}$ ($u_2^{(-)}$) and $r_<$ is the lesser of r or R. The amplitude (21) can be further simplified depending upon the choice of coordinate axis. The two most common choices place the z axis (a) along the direction of the incident electron, or (b) along the momentum transfer $\vec{q} = \vec{k}_i - \vec{k}_1$ ($\vec{k}_i$ and $\vec{k}_1$ define the scattering plane). With the latter choice, PWBA cross sections exhibit a particularly simple behavior. We shall examine the cross sections in both reference frames.

1. z axis along $\vec{k}_i$

For the choice of the z axis along $\vec{k}_i$, we chose the y axis along $\vec{k}_i \times \vec{k}_1$. With this choice of reference frame, it may be shown after some angular momentum algebra that the triple-differential direct amplitude is given by

$$f = (4\pi^3)^{-1} (k_i k_1 k_2)^{-1/2} \times \sum_{l_2 m_2} D^{l_o m_o}_{l_2 m_2}(\theta_f) P^{|m_2|}_{l_2}(\theta_s) \exp(i m_2 \phi_s) , \quad (24)$$

where

$$D^{l_o m_o}_{l_2 m_2}(\theta_f) = \sum_{l_1 l l_i} G^{l, m_o - m_2, m_2}_{l_o l_i l_1 l_2} I^{k_i k_1 k_2}_{l_o l_i l_1 l_2} P^{|m_o - m_2|}_{l_1}(\theta_f) , \quad (25)$$

with

$$G^{lm_1m_2}_{l_o l_i l_1 l_2} = (2l_i+1)(2l_1+1)(2l_o+1)^{1/2}(2l+1)^{-1} i^{l_o+l_i-l_1-l_2}$$
$$\times (-1)^{(2m_2-m_o+|m_1|+|m_2|+|m_1+m_2-m_o|)/2} C(l_i l_1 l; m_1+m_2-m_o, -m_1, m_2-m_o)$$
$$\times C(l_i l_1 l; 0) C(l_o l l_2; m_o, m_2-m_o, m_2) C(l_o l l_2; 0) R^{|m_1|}_{l_1} R^{|m_2|}_{l_2} R^{|m_1+m_2-m_o|}_{l_i}, \quad (26)$$

while the exchange amplitude is given by

$$g = (4\pi^3)^{-1}(k_i k_1 k_2)^{-1/2}$$
$$\times \sum_{l_1 m_1} E^{l_o m_o}_{l_1 m_1}(\theta_f) P^{|m_1|}_{l_1}(\theta_s) \exp(i m_1 \phi_s), \quad (27)$$

where

$$E^{l_o m_o}_{l_1 m_1}(\theta_f) = \sum_{l_2 l l_i} G^{l, m_1, m_o-m_1}_{l_o l_i l_1 l_2} I^{k_i k_2 k_1}_{l_o l_i l_1 l_2} P^{|m_o-m_1|}_{l_2}(\theta_f), \quad (28)$$

and where

$$R^{|m|}_l = [(l-|m|)!/(l+|m|)!]^{1/2}. \quad (29)$$

These formulas exhibit some simple properties for electrons ejected from an s shell ($l_o = m_o = 0$). For this case, it can be seen that

$$D^{00}_{l_2 m_2} = D^{00}_{l_2 -m_2} \text{ and } E^{00}_{l_1 m_1} = E^{00}_{l_1 -m_1}. \quad (30)$$

If this fact is used in (24) and (27), one sees that the amplitudes for $\pm\phi_s$ are the same, reflecting the expected mirror symmetry about the scattering plane for ionization of s shells.

Since the PWBA continues to provide a popular reference for this type of calculation, we have examined the direct amplitudes for the case in which the wave functions for the incident electron and fast final-state continuum electron are plane waves. With this simplification, the direct amplitude in the PWBA reduces to

$$f^{\text{Born}} = (k_i k_1 k_2^{-1})^{1/2}(4\pi^3 q^2)^{-1} \sum_{lm} A^{l_o m_o}_{lm}(\alpha) P^{|m|}_l(\theta_s) e^{im\phi_s}, \quad (31)$$

where

$$A^{l_o m_o}_{lm}(\alpha) = \sum_\lambda (2l_o+1)^{1/2}(2\lambda+1)(-1)^{(m_o+|m|+|m-m_o|)/2} i^{l_o-l+\lambda}$$
$$\times R^{|m|}_l R^{|m-m_o|}_\lambda H^{k_2 q}_{l\lambda l_o} C(l_o \lambda l; m_o, m-m_o, m) C(l_o \lambda l; 0) P^{|m-m_o|}_\lambda(\alpha), \quad (32)$$

and where

$$H^{k_2 q}_{l\lambda l_o} = \int_0^\infty \beta^2_{l_2}(k_2, r) j_\lambda(qr) U_{l_o}(r)\, dr. \quad (33)$$

Here $q^2 = |\vec{k}_i - \vec{k}_1|^2$, α is the angle between $\vec{k}_i$ and $\vec{q}$, and $j_\lambda(qr)$ is a spherical Bessel function.

2. z axis along $\vec{q}$

For the choice of the z axis along $\vec{q}$, the y axis remains along $\vec{k}_i \times \vec{k}_1$. This situation represents a rotation of our previous results about the y axis. This rotation makes the DWA formulas more complicated and the PWBA formulas simpler. The DWA direct amplitude may be shown to be given by (24), where

$$D^{l_o m_o}_{l_2 m_2}(\theta_f) = \sum_{l_1 m_1 l_i l} G^{l m_1 m_2}_{l_o l_i l_1 l_2} I^{k_i k_1 k_2}_{l_o l_i l_1 l_2}$$
$$\times P^{|m_1|}_{l_1}(\gamma) P^{|m_1+m_2-m_o|}_{l_i}(\alpha). \quad (34)$$

The DWA exchange amplitude is given by (27), where

$$E^{l_o m_o}_{l_1 m_1}(\theta_f) = \sum_{l_2 m_2 l l_i} G^{l m_1 m_2}_{l_o l_i l_1 l_2} I^{k_i k_2 k_1}_{l_o l_i l_1 l_2}$$
$$\times P^{|m_2|}_{l_2}(\gamma) P^{|m_1+m_2-m_o|}_{l_i}(\alpha). \quad (35)$$

Here γ is the angle between $\vec{k}_1$ and $\vec{q}$. In the limit of $\alpha = 0$, (34) and (35) reduce to (25) and (28). The amplitudes (34) and (35) satisfy the symmetry relationship (30).

It can be shown that the PWBA direct amplitude may be expressed in this coordinate system by (31) with $m = m_o$ and $\alpha = 0$. For scattering from an s shell, this amplitude has no ϕ_s dependence. As a result, the PWBA predicts that the triply differential cross sections will have azimuthal symmetry about the $\vec{q}$ axis. The DWA amplitudes do not formally exhibit this symmetry.

B. Numerical procedure

The primary numerical problem associated with finding the amplitudes lies in evaluating the radial overlap integrals (22). The two major problem areas are large radii and large l values. Fortunately, the direct amplitude in these two regions

can be reduced to analytic expressions. For radii larger than the extent of the atomic wave function and potential (R_0), the form factor (23) can be written

$$F^{k_2}_{l_1 l_2}(R)_{R>R_0} = B^{k_2}_{l_0 l_1 l_2}/R^{l+1}, \tag{36}$$

where

$$B^{k_2}_{l_0 l_1 l_2} = \int_0^{R_0} \beta^2_{l_2}(k_2, r) r^l U_{l_0}(r)\, dr. \tag{37}$$

For high-energy projectiles, the incident and fast electrons will asymptotically be moving in a field-free region. In this region, the distorted waves will be phase-shifted spherical Bessel functions. As a result both β^l and β^i in the direct amplitude can be expressed in the region $r>R_0$ as

$$\beta_l(kr) = kr\, j_l(kr) + c_l[kr\, j_l(kr) + ikr\, y_l(kr)], \tag{38}$$

where j_l (y_l) is a regular (irregular) spherical Bessel function, and c_l gives the effect of the atomic potential on the distorted wave. For scattering from a zero potential (PWBA), $c_l = 0$. If these expressions are inserted into (22), the contribution to the radial overlap integrals for $R>R_0$ can be expressed in terms of sine and cosine integrals by making the standard sine and cosine expansions of the spherical Bessel functions. The algebra and results are straightforward but tedious and will not be presented here. For this calculation, R_0 was taken to be about $36a_0$.

The radial overlap integral may also be simply evaluated for large angular momenta. The centrifugal barrier provides a region around the nucleus into which the electron effectively may not penetrate. The range of this barrier increases with increasing angular momenta. For high angular momenta, the effective range of the barrier becomes larger than the effective range of the atomic potential. Under these circumstances, $c_l \simeq 0$ and (22) may be evaluated analytically for all radii. Under these circumstances, the radial overlap integral becomes

$$I^{k_i k_1 k_2}_{l_0 l_i l_1 l_2} = B^{k_2}_{l_0 l_1 l_2} \pi 2^{-l-1} k_i^{l-l_1-1} k_1^{l_1+1} \frac{\Gamma(\frac{1}{2}(l_1 + l_i - l + 2))}{\Gamma(l_1 + 1\frac{1}{2})\,\Gamma(\frac{1}{2}(l_i + l - l_1 + 1))}$$
$$\times F(\tfrac{1}{2}(l_1 + l_i - l + 2), \tfrac{1}{2}(l_1 - l_i - l + 1); l_1 + 1\tfrac{1}{2}; (k_1/k_i)^2), \tag{39}$$

where Γ is the gamma function and F is a hypergeometric function. It should be noted that this is the limit in which the DWA amplitude goes over to the corresponding PWBA amplitude. For the present calculation, the DWA direct amplitude approached the PWBA amplitude for l values in the neighborhood of 30. Obviously, this procedure cannot be used for the exchange amplitude since the electron roles are interchanged.

For the results presented here, the atomic potentials were obtained using the Hartree-Fock program of Froese-Fischer.[21] The asymptotically neutral Hartree-Fock potential was used to calculate the continuum eigenfunctions for the fast electron. The ionic potential was obtained by removing one electron from neutral helium while leaving the remaining bound-state wave function unchanged. To insure orthogonality between the bound-state wave function and the slow continuum electron wave function, both wave functions were calculated as eigenfunctions of the ionic potential.

Previous calculations have been made for this process using the DWA method. The dissertation of Baluja[22] (directed by one of us, W.N.S.) dealt only with incident electron energies of 256 eV and used only two partial waves for the ejected electron, even for ejected electron energies as high as 50 eV. Two partial waves are inadequate; we use seven in the present work. This calculation neglected exchange.

More recently, an improvement on the dissertation of Baluja has been published by Baluja and Taylor[12] from the point of view of a first-order approximation to the many-body theory. In this calculation, three partial waves were used for the slow electron at energies of 3 eV or less, five partial waves were used at higher ejection energies, and numerical integrations were performed up to a radius of $10a_0$. In the work reported in the present paper, the following parameters have been used: (i) direct calculation: slow electron, 7 partial waves; incident electron, 100 partial waves; and numerical integration to infinity using the analytic method discussed earlier; (ii) exchange calculation: fast electron, 25 partial waves; incident electron, 40 partial waves; and numerical integration to $72a_0$. We have compared the present parameters with the parameters used by Baluja and Taylor. The parameters used in the present calculation gave direct and exchange cross sections that had converged better. Interestingly, use of the less-well-converged parameters gave cross sections of different magnitude but similar shape. We could not make a quantitative comparison with the work of Baluja and Taylor since their paper does not give the magnitudes of the angular distributions. We have attempted to make a comparison by normalizing their cross sections to our values at the forward peak. This procedure reveals that the shape of their cross sections is

almost identical to ours for 256-eV incident electrons.

The computer code developed for this calculation can be used to perform a PWBA, CPBA, or DWA calculation, depending upon the input parameters. This versatility provided several options for checking the code. The code was checked in the following ways: (i) PWBA ionization of hydrogen was calculated and compared with an analytic expression given by Landau and Lifshitz[23]; (ii) PWBA ionization of helium was compared with a corresponding calculation performed using a separate independent code[24]; and (iii) CPBA calculations were compared with the corresponding calculations performed by Geltman.[11] In each case, excellent agreement was found.

III. RESULTS

The results of the calculation for the scattering plane are compared with the experimental data of Ehrhardt *et al.*,[1,2] and with previous theoretical calculations of Geltman[11] and Robb *et al.*[9] in the first four figures. The calculation of Geltman was performed in the CPBA and the calculation by Robb *et al.*, was performed in the PWBA. In that PWBA calculation, the incident and scattered electron wave functions were represented as plane waves, while configuration-interaction wave functions were used to describe the initial-bound-target state and close-coupling wave functions were used to describe the final-continuum-target state. Exchange was neglected. The present Born curves in the figures were obtained using the distorted-wave code by setting the potential seen by the incident and faster final-state continuum electron equal to zero and by setting the exchange amplitude equal to zero.

Since the experimental data are unnormalized, we have arbitrarily normalized the experimental data to the distorted-wave curve at the forward peak. From the first two figures, it is seen that for a 256.5-eV incident electron, the DWA calculation is in fairly good agreement with the experimental data. The largest deviation between the data and the DWA calculation is seen for the higher energy transferred and for larger angles of observation for the fast electron. Under these circumstances, the forward lobe in the experimental

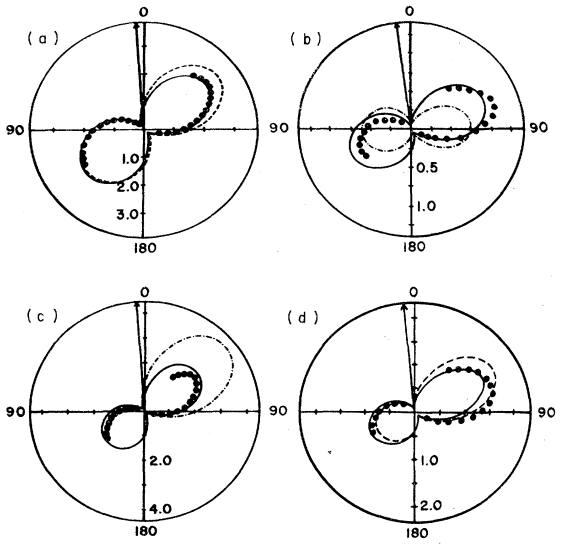

FIG. 1. Triple-differential cross sections for 256.6-eV electron-impact ionization of helium in units of a_0^2/sr^2 Ry. The experimental data are those of Ehrhardt *et al.*, the solid curves are the present DWA calculations including exchange, and the dashed curves are the present PWBA calculations. The angle of observation for the faster electron θ_f and the energy of the slower electron E_s are as follows: (a) $\theta_f = 4°$ and $E_s = 1.5$ eV; (b) $\theta_f = 7°$, $E_s = 1.5$ eV, and the dot-dashed curve is the CPBA calculation of Geltman; (c) $\theta_f = 4°$, $E_s = 3$ eV, and the dot-dashed curve is the PWBA calculation of Robb *et al.* The DWA and PWBA calculations are the same within plotting accuracy at the backward lobe; (d) $\theta_f = 6°$ and $E_s = 3$ eV.

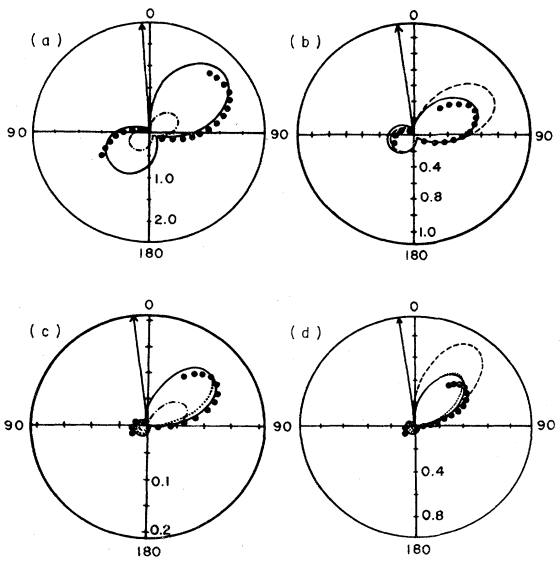

FIG. 2. Triple-differential cross sections for 256.5-eV electron-impact ionization of helium in units of a_0^2/sr^2 Ry. The experimental data are those of Ehrhardt *et al.*, the solid curves are the present DWA calculations including exchange, the dotted curves are the DWA results without exchange, the dashed curves are the present PWBA results, and the dot-dashed curves are the CPBA calculations of Geltman. The angle of observation for the faster electron θ_f and energy of the slow electron E_s are as follows: (a) $\theta_f = 4°$ and $E_s = 6$ eV; (b) $\theta_f = 8°$ and $E_s = 6$ eV; (c) $\theta_f = 8°$ and $E_s = 35$ eV; (d) $\theta_f = 8°$ and $E_s = 50$ eV.

data seems to be rotated to larger angles. On curves c and d of Fig. 2, the DWA cross section that would be obtained by setting the exchange term equal to zero is also plotted. It is interesting to note that the exchange term rotates the DW lobe towards the data. This observation supports the idea that correlation effects are responsible for the shift of the lobe.[7,12]

Of special interest is the Born approximation calculation by Robb *et al.*, shown in Fig. 1(c). In this calculation, the bound and continuum wave functions for the slow electron are superior to the corresponding wave functions used in the present calculation. The important difference between the two calculations lies in the treatment of the incident electron—a plane wave for a PWBA calculation and an elastic scattering wave function in a DWA calculation. These results indicate that it is not useful to treat one aspect of the scattering problem (electron ejection) highly accurately while treating another aspect (incident electron) in an elementary fashion. Comparison of the DWA curves with the present Born curves provides a direct comparison of the effect of distortion on the incident electron, since the slow-electron wave functions were the same in both calculations.

Figures 3 and 4 provide similar comparisons for incident electrons of 80.5 eV and 50 eV. The agreement with data is significantly worse at these lower energies. As one would expect and as may be seen from the figures, the effects of exchange are more significant at these parameters. At these lower energies, the energy difference between the fast and slow electron can become small. This situation brings into question the basic model of the process used here where the fast electron "sees" an effective neutral atom in both the initial and final channels and the slow electron "sees" a final-state ion. Various proposals have been made to combat this problem ranging from time arguments[12] to effective charges.[19] We will explore this problem in more depth in a later publication.

Figures 5–7 present three-dimensional surface plots for the DWA cross sections to illustrate the behavior of the cross sections off the scattering plane. The horizontal axis corresponds to the scattering angle θ_s measured relative to the direction of the incident beam while the oblique axis corresponds to the azimuthal angle ϕ_s. The half of the scattering plane containing the scattered fast electron corresponds to $\phi_s = 0°$ and the other half of the scattering plane corresponds to $\phi_s = 180°$. As was pointed out earlier, cross sections for ϕ between 180° and 360° are mirror symmetrical about those shown in the figures.

From Figs. 5 and 6, one can see an evolution of the cross section for 256.5-eV incident electrons as the energy of the slower electron is increased. With increasing energy for the slower electron,

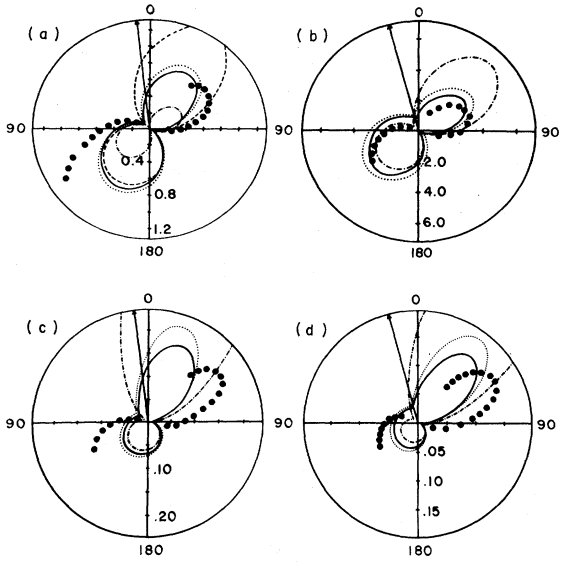

FIG. 3. Triple-differential cross sections for 80.5-eV electron-impact ionization of helium in units of a_0^2/sr^2 Ry. The experimental data are those of Ehrhardt *et al.*, the solid curves are the present DWA results including exchange, and the dotted curves are the DWA results without exchange. The angle of observation for the faster electron θ_f and energy of the slower electron E_s are as follows: (a) $\theta_f = 7°$, $E_s = 2.5$ eV, the dot-dashed curve is the CPBA calculation of Geltman, and the dashed curve is the present PWBA; (b) $\theta_f = 15°$, $E_s = 2.5$ eV, and the dot-dashed curve is the present PWBA; (c) $\theta_f = 7°$, $E_s = 15.5$ eV, and the dot-dashed curve is the present PWBA; (d) $\theta_f = 15°$, $E_s = 15.5$ eV, and the dot-dashed curve is the present PWBA.

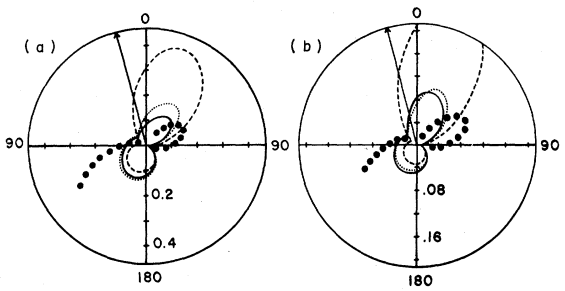

FIG. 4. Triple-differential cross sections for 50-eV electron-impact ionization of helium in units of a_0^2/sr^2 Ry. The experimental data are those of Ehrhardt *et al.*, the solid curves are the present DWA results including exchange, the dotted curves are the DWA results without exchange, and the dashed curves are the present PWBA. The angle of observation for the faster electron θ_f and energy of the slower electron E_s are as follows: (a) $\theta_f = 15°$ and $E_s = 5.5$ eV; (b) $\theta_f = 15°$ and $E_s = 10.5$ eV.

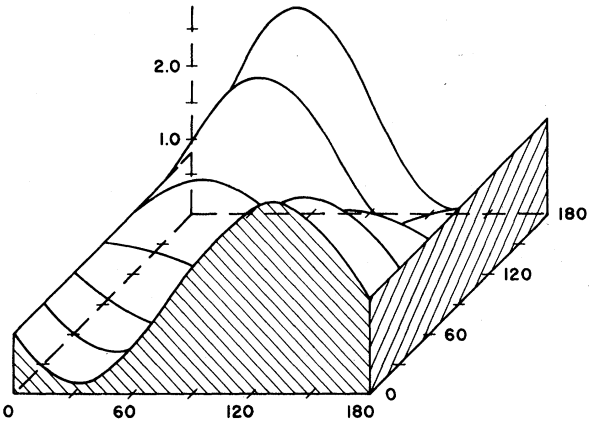

FIG. 5. Three-dimensional DWA triple-differential cross sections for 256.5-eV electron-impact ionization of helium in units of a_0^2/sr^2 Ry. The angle of observation for the faster electron $\theta_f = 4°$ and the energy of the slower electron $E_s = 1.5$ eV. The horizontal axis corresponds to the polar scattering angle θ_s in degrees and the oblique axis corresponds to the azimuthal scattering angle ϕ_s.

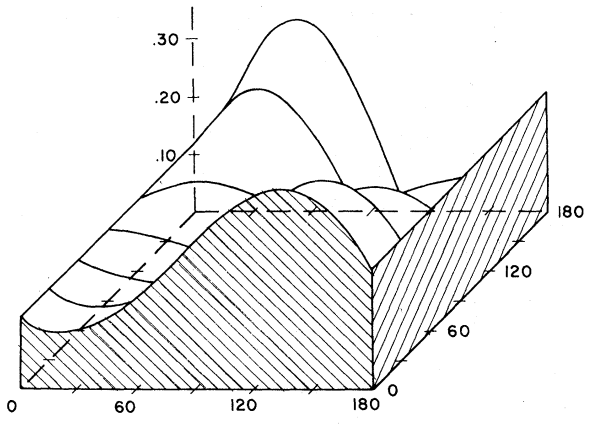

FIG. 7. Same as Fig. 5 except here the energy of the incident electron is 80.5 eV, $\theta_f = 15°$, and $E_s = 2.5$ eV.

the backward lobe diminishes with increasing ϕ and the forward lobe starts to build up until the cross sections begin to take on the shape one would expect for a classical binary collision (Fig. 6). Figure 7 illustrates typical results for 80.5-eV incident electrons. At lower energies, the relative effect of the backward lobe is generally more pronounced.

Figures 8–10 illustrate the DWA cross sections expressed relative to a coordinate system whose z axis is along the momentum-transfer direction. As discussed previously, the cross sections in the Born approximation are azimuthally symmetric about this axis. In these figures, the angle θ is

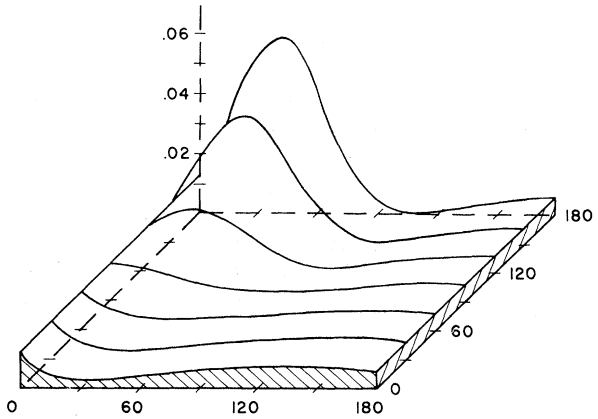

FIG. 6. Same as Fig. 5 except here $\theta_f = 8°$ and $E_s = 50$ eV.

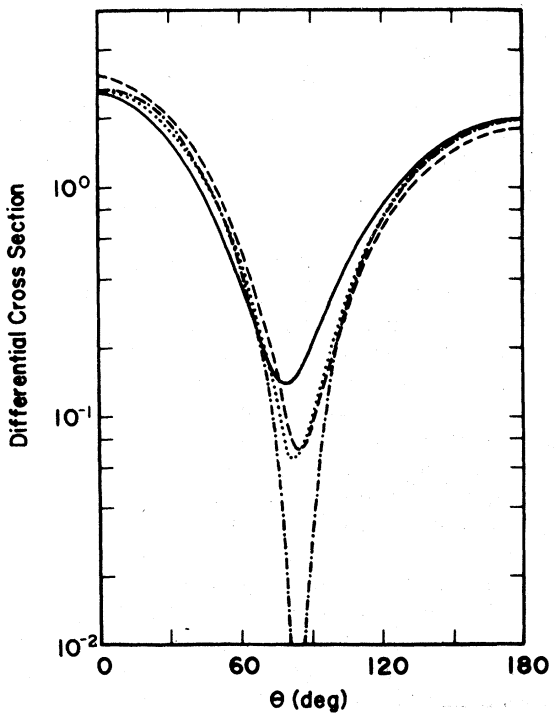

FIG. 8. Distorted-wave triple-differential cross sections for 256.5-eV electron-impact ionization of helium in units of a_0^2/sr^2 Ry expressed relative to the $\vec{q}$ direction. The horizontal axis corresponds to the polar scattering angle θ_s, the solid curve corresponds to the azimuthal angle $\theta_s = 0$, the dotted curve represents the polar angle $\phi_s = 90°$, the dot-dashed curve represents $\phi_s = 180°$, and the dashed curve is the present PWBA results. The angle of observation for the faster electron $\theta_f = 4°$ and the energy of the slower electron $E_s = 3$ eV.

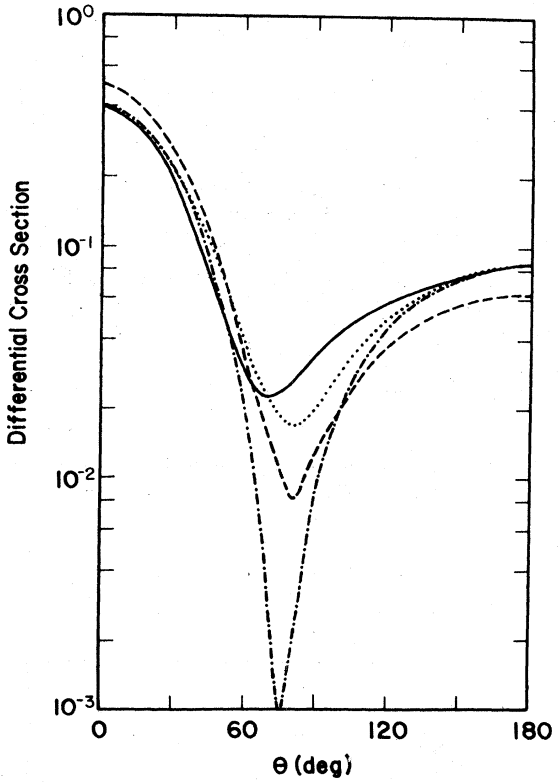

FIG. 9. Same as Fig. 8 except here $\theta_f = 8°$ and $E_s = 20$ eV.

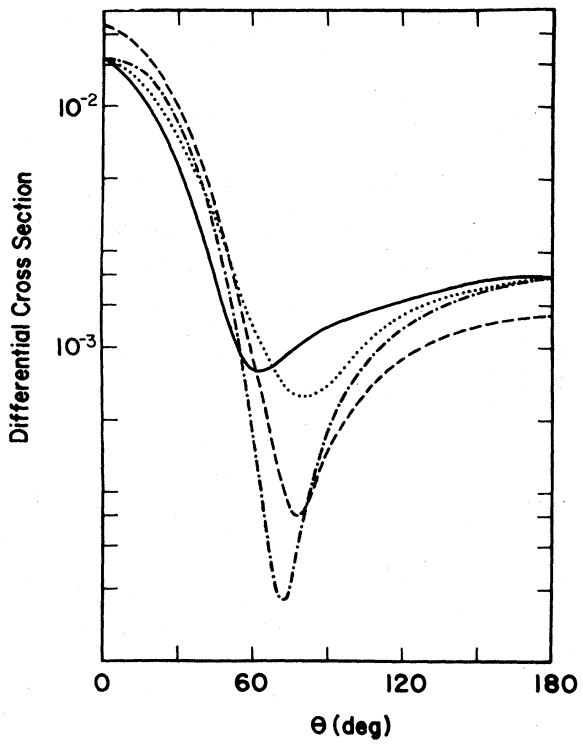

FIG. 10. Same as Fig. 8 except here $\theta_f = 8°$ and $E_s = 50$ eV.

measured relative to the z axis and the half of the scattering plane containing the faster electron again corresponds to $\phi_s = 0°$. The Born curve was calculated using the DWA code. In each figure, DWA cross sections are presented for the scattering plane ($\phi_s = 0°$ and 180°) and for a plane perpendicular to the scattering plane.

It is not surprising that these figures show that the DWA approximation does not exhibit the azimuthal symmetry exhibited by the Born approximation. More interesting is the fact that while the DWA calculation gives results significantly different from the Born calculation, the DWA results do indicate a tendency for this symmetry except for angles near the minimum in the cross section. This symmetry becomes less visible for larger scattering angles of the faster electron and for higher energy transferred. The calculations represented in Figs. 8–10 do not include exchange.

In conclusion, we have calculated triple-differential cross sections for electron-impact ionization of helium in the distorted-wave approximation. These cross sections were in better agreement with the 256.5-eV data than were the corresponding Born or Coulomb-projected Born cross sections. Since these different approaches can give cross sections of greatly varying magnitudes, absolute measurements would be extremely valuable. The DWA cross sections do not exhibit azimuthal symmetry about the momentum-transfer direction, and the lack of symmetry is most pronounced near the minimum in the cross section or for higher-energy transfers.

ACKNOWLEDGMENTS

The authors would like to thank J. K. Berkowitz and B. M. Bakken for programming assistance and R. W. Lutz and his staff at the Drake Computing Center for technical assistance. Helpful discussions with M. Inokuti and Y. K. Kim are gratefully acknowledged.

*Work supported by the Research Corporation.

[1]H. Ehrhardt, K. H. Hesselbacher, K. Jung, and K. Willmann, J. Phys. B 5, 1559 (1972).
[2]H. Ehrhardt, K. H. Hesselbacher, K. Jung, M. Schulz, and K. Willmann, J. Phys. B 5, 2107 (1972).
[3]H. Ehrhardt, K. H. Hesselbacher, K. Jung, E. Schubert, and K. Willmann, J. Phys. B 7, 69 (1974).
[4]K. Jung, E. Schubert, H. Ehrhardt, and D. A. L. Paul, J. Phys. B 9, 75 (1976).
[5]S. T. Hood, I. E. McCarthy, P. J. O. Teubner, and E. Weigold, Phys. Rev. A 8, 2494 (1973).
[6]E. Wiegold, in Proceedings of the Second International Conference on Inner Shell Ionization Phenomena, Invited Papers, Freiburg, W. Germany, 1976 (unpublished), p. 367.
[7]A. Salin, J. Phys. B 6, L34 (1973).
[8]V. L. Jacobs, Phys. Rev. A 10, 499 (1974).
[9]W. D. Robb, S. P. Roundtree, and T. Burnett, Phys. Rev. A 11, 1193 (1975).
[10]T. Burnett, S. P. Roundtree, G. Doolen, and W. D. Robb, Phys. Rev. A 13, 626 (1976).
[11]S. Geltman, J. Phys. B 7, 1994 (1974).
[12]K. L. Baluja and H. S. Taylor, J. Phys. B 9, 829 (1976).
[13]D. H. Madison and W. N. Shelton, Phys. Rev. A 7, 499 (1973).
[14]D. H. Madison and W. N. Shelton, Phys. Rev. A 7, 514 (1973).
[15]R. V. Calhoun, D. H. Madison, and W. N. Shelton, Phys. Rev. A 14, 1380 (1976).
[16]M. Inokuti, Rev. Mod. Phys. 43, 297 (1971).
[17]D. H. Madison and E. Merzbacher, in *Atomic Inner-Shell Processes*, edited by B. Craseman (Academic, New York, 1975), Chap. 1.
[18]D. M. Brink and G. R. Satchler, *Angular Momentum* (Oxford University, London, 1968).
[19]M. R. H. Rudge, Rev. Mod. Phys. 40, 564 (1968).
[20]A. Messiah, *Quantum Mechanics* (Wiley, New York, 1968), Chap. XI.
[21]C. Froese-Fischer, Comput. Phys. Commun. 4, 107 (1972).
[22]K. L. Baluja, dissertation, Florida State University, 1973 (unpublished).
[23]L. D. Landau and E. M. Lifshitz, *Quantum Mechanics* (Pergamon, Oxford, 1965), p. 579.
[24]D. H. Madison, Phys. Rev. A 8, 2449 (1973).